

MIM-Based GAN: Information Metric to Amplify Small Probability Events Importance in Generative Adversarial Networks

Rui She, Pingyi Fan, *Senior Member, IEEE*

Abstract

In terms of Generative Adversarial Networks (GANs), the information metric to discriminate the generative data from the real data, lies in the key point of generation efficiency, which plays an important role in GAN-based applications, especially in anomaly detection. As for the original GAN, there exist drawbacks for its hidden information measure based on KL divergence on rare events generation and training performance for adversarial networks. Therefore, it is significant to investigate the metrics used in GANs to improve the generation ability as well as bring gains in the training process. In this paper, we adopt the exponential form, referred from the information measure, i.e. MIM, to replace the logarithm form of the original GAN. This approach is called MIM-based GAN, has better performance on networks training and rare events generation. Specifically, we first discuss the characteristics of training process in this approach. Moreover, we also analyze its advantages on generating rare events in theory. In addition, we do simulations on the datasets of MNIST and ODDS to see that the MIM-based GAN achieves state-of-the-art performance on anomaly detection compared with some classical GANs.

Index Terms

Generative Adversarial Networks, Message Importance Measure (MIM), Information Measure, Rare Events Generation, Anomaly Detection

I. INTRODUCTION

In order to produce deceptive generative data, GANs are proposed as a kind of efficient approach [1]. Especially, complex or high-dimensional distributions are handled pretty well by GANs [2], [3]. Actually,

R. She and P. Fan are with Beijing National Research Center for Information Science and Technology and the Department of Electronic Engineering, Tsinghua University, Beijing, 100084, China (e-mail: sher15@mails.tsinghua.edu.cn; fpy@tsinghua.edu.cn).

the core idea of GANs is to generate samples whose distribution approximates the target distribution as much as possible. In practice, GANs are applied in many scenarios [4]–[8], such as images reconstruction, autonomous driving models, and samples augmentation. In theory, the framework of GANs consists of a generator network and a discriminator network, which respectively minimizes and maximizes the distinction between the real data distribution and the generated distribution. In this case, the information distance (which is Jensen-Shannon divergence in the original GAN) plays a vital role in the generative adversarial process. On one hand, the performance of training process depends on the information distance. On the other hand, the efficiency of generative data (especially for rare events data) is related to this metric. Therefore, it is worth investigating the information distance and its corresponding objective function of GANs to improve the training process and GAN-based applications such as anomaly detection.

A. Different information distances for GANs

Considering the information distance choice of GANs, there are some literatures discussing how the different distances make impacts on the optimization of objective functions in the generative process. In terms of the original GAN, it optimizes the Jensen-Shannon divergence (which is based on Kullback-Leibler (KL) divergence) to generate samples. Similar to the original generative model, the affine projected GAN (or AffGAN for short) is also discussed to minimize the KL divergence between the two distributions (namely, the real data distribution and the generative one), which is suitable for Maximum a Posterior (MAP) inference with respect to image super-resolution [9]. However, there exists faultiness for KL divergence as a metric in the objective function of GANs, which performs in training stability and efficiency. To make up for this, some other information distances are considered to replace the original KL divergence as follows.

As a kind of refined GAN, Energy-Based Generative Adversarial Network (EBGAN) based on the total variation, allocates lower energies to the adjacent regions of the real data manifold and larger energies to the rest regions. Compared with the original GAN, the EBGAN performs more stable in the training process [10]. Moreover, to overcome the vanishing gradients problem caused by the loss function of the original GAN, Least Squares Generative Adversarial Networks (LSGAN) is proposed, which is to minimize the Pearson χ^2 divergence as the objective function [11]. Another distance, Chi-Squared distance, is also used to design the Fisher GAN which constrains the second order moments of the critic and leads to train the adversarial networks in a stable way [12]. To extend GANs into a general way, f -divergence is discussed to train generative models where the benefits of different information distances belonging

to f -divergence are investigated with respect to the training complexity and the quality [13]. In addition, Wasserstein-GAN (WGAN) is proposed to estimate Earth Mover distance (EM distance) continuously, which overcomes the training imbalance problem of GANs. Furthermore, WGAN-GP, a kind of refined WGAN, is introduced to enforce the Lipschitz constraint, which enables to train neural networks more stably without any hyper-parameter tuning [14], [15].

In brief, it is a popular research direction to introduce a promising information distance into GANs to see whether there exist performance gains on training process.

B. Generative efficiency for rare events

Anomaly detection is a common problem with real-world significance [16]–[18]. Inspired by the success of neural networks, GANs are considered as an efficient approach to detect anomalies which are regarded as rare events from the perspective of occurrence probability. Particularly, the original GAN has played great roles in anomalous natural and medical images detection [19], [20].

In terms of the anomaly detection with GANs, the method is to regard the samples as anomalies depending on if the appropriate representations of samples in the latent space of generator are found. Specifically, the generator learns an approximate distribution of the training data, in which there are more normal events (hardly ever with anomalies). Thus, for a normal testing sample, it is probable to find a point in the latent space of GANs similar to this one, while for an anomalous sample it is not. Based on this idea, there exist works using GANs in anomaly detection as follows [21]–[23].

A method called AnoGAN using normal data to train the original GAN [21], defines an anomaly score to distinguish the generative samples (namely normal samples) and the anomalous samples. Moreover, another similar method learns two generators by training a conditional GAN to reconstruct normal frames (with low reconstruction loss) and rare frames (with high reconstruction loss) [24]. Besides, an unsupervised feature learning framework, Bidirectional Generative Adversarial Networks (BiGAN) is also proposed to train the networks with normal data and combine the reconstruction loss and discriminator loss as the score function to detect anomalies [25]. Furthermore, other GAN-based anomaly detection approaches such as Generative Adversarial Active Learning (GAAL) and fast AnoGAN (or f-AnoGAN) are designed by making use of the prior information during the adversarial training process [4], [26].

Moreover, the discriminator to distinguish the real samples and fake ones is also applied reasonably to detecting anomalies. In particular, once the training process is converged, the discriminator can not cope

with the testing data that is unlike the training data (which corresponds to the anomalous data) [27], [28]. As a result, it is feasible to combine the discriminator and generator of GANs to detect anomalies.

However, since the rare events (including anomalies) play a small part in the whole dataset, the generative data more likely belongs to the main part of normal data rather than small probability data. In terms of the original GAN, the proportion of rare events in the objective function is not large enough compared with that for normal events, which makes an effect on rare events generation.

In addition, as for the original GAN, there exist drawbacks in convergence rate, sensitivity and stability of training process. Besides, there are few literatures to investigate the improvements for objective functions (related to information distances) from the perspective of rare events generation, which is also beneficial for GAN-based anomaly detection. Therefore, we have an opportunity to investigate a new information metric to improve the original GAN-based rare events generation and anomaly detection.

In this work, we introduce the idea of Message Importance Measure (MIM) into the GANs and propose a MIM-based GAN method to detect anomalies. In this case, there are improvements in the objective function for training process and rare events generation. Furthermore, experiments on real datasets are taken to compare our method with other classical methods.

C. Contributions and organization

Here, we provide the contributions and organization for this work.

- At first, by resorting to the idea of Message Importance Measure (MIM), MIM-based GAN is designed for probability distribution learning. As well, some characteristics of this GAN are also discussed.
- Then, the proposed MIM-based GAN highlights the proportion of rare events in the objective function, which reveals its advantages on rare events generation in theory.
- At last, MIM-based GAN performs better in anomaly detection than some other GANs. Specifically, the experiments (based on artificial dataset and real datasets) are designed to intuitively show the different performance on the results of detection.

In addition, the organization of the rest part is provided as follows. In Section II, we propose the MIM-based GAN by resorting to the idea of MIM and discuss its major properties in the training process. In Section III, we theoretically analyze the effect of rare events on generators and discuss the its corresponding anomaly detection. Section IV compare several GANs with MIM-based GAN in the experiments of anomaly detection. At last, this work is concluded in the Section V.

II. MODEL OF MIM-BASED GAN

A. Overview of GANs

In terms of GANs, the essential idea is to train two artificial neural networks to generate the data, which has the same distribution as the real data distribution. To do this, the objective functions of GANs play vital roles in the two-player game for the two neural networks which are regarded as the discriminator and generator respectively. In fact, there exists a general form of objective function optimization for GANs, which is described as

$$\min_G \max_D L(D, G), \quad (1)$$

where $L(D, G)$ denotes the objective function given by

$$\begin{aligned} L(D, G) &= \mathbb{E}_{\mathbf{x} \sim \mathbb{P}}[f(D(\mathbf{x}))] + \mathbb{E}_{\mathbf{z} \sim \mathbb{P}_z}[g(D(G(\mathbf{z})))] \\ &= \mathbb{E}_{\mathbf{x} \sim \mathbb{P}}[f(D(\mathbf{x}))] + \mathbb{E}_{\mathbf{x} \sim \mathbb{P}_{g\theta}}[g(D(\mathbf{x}))], \end{aligned} \quad (2)$$

in which $f(\cdot)$ and $g(\cdot)$ are functions, D is the discriminator, G is the generator (D and G are both represented by neural networks), \mathbf{x} and \mathbf{z} denote the input for D and G respectively, as well as \mathbb{P} , $\mathbb{P}_{g\theta}$ and \mathbb{P}_z are distributions for real data, generative data and input data of generator.

B. MIM-based GAN and Corresponding Characteristics

According to the comparison for MIM and Shannon entropy [29]–[31], it is known that the exponential function used to replace the logarithmic function, has more positive impacts on the rare events processing from the viewpoint of information metrics. Furthermore, based on the exponential function, an information distance, Message Identification (M-I) divergence is proposed to gain the greater effect of amplification on detecting outliers than Kullback-Leibler (KL) divergence (which is based on logarithmic function) [32]. As a result, exponential function with different properties from logarithmic function makes differences on information characterization. In this regard, there may exist potential advantages to introduce exponential function into the original GAN which incorporates the logarithmic function in the objective function.

By virtue of the essential idea of MIM and the convexity of exponential function, we have the modified objective function of GANs as follows

$$\begin{aligned} L_{\text{MIM}}(D, G) &= \mathbb{E}_{\mathbf{x} \sim \mathbb{P}}[\exp(1 - D(\mathbf{x}))] + \mathbb{E}_{\mathbf{z} \sim \mathbb{P}_z}[\exp(D(G(\mathbf{z})))] \\ &= \mathbb{E}_{\mathbf{x} \sim \mathbb{P}}[\exp(1 - D(\mathbf{x}))] + \mathbb{E}_{\mathbf{x} \sim \mathbb{P}_{g\theta}}[\exp(D(\mathbf{x}))], \end{aligned} \quad (3)$$

whose notations are the same as those in $L(D, G)$ (mentioned in the Eq. (2)).

Similar to the original GAN, the modified objection function Eq. (3) also plays the two-player optimization game with respect to D and G as follows

$$\max_G \min_D L_{\text{MIM}}(D, G), \quad (4)$$

and the corresponding adversarial networks are referred to as *MIM-based GAN*. Essentially, the goal of the MIM-based GAN is to train an optimal couple of discriminator and generator to learn the real data distribution, which is as same as that in the original GAN. In particular, the principle of MIM-based GAN are detailed as follows.

On one hand, the network of discriminator D is designed to assign the real label (usually “1”) and fake label (usually “0”) to the real data and generative data (from the generator G). In this case, the input pairs for D consist of data (namely real data and generative data) and labels (containing real labels and fake labels). On the other hand, the network of generator G tends to output imitative data more like the real data, whose goal is to deceive the discriminator. In other words, the discriminator D is misled by the generator G to make the similar decision for the generative data and real data. In this case, the input pairs of G are data z (randomly drawn from a latent space) and real labels. Furthermore, the loss functions of D and G are given by Eq. (4) which leads the two networks to update their weight parameters by means of back propagation. Finally, by selecting neural networks structures for D and G , the training process of MIM-based GAN is completed.

Then, some fundamental characteristics of MIM-based GAN are discussed as follows.

1) *Optimality of $\mathbb{P} = \mathbb{P}_{g_\theta}$:*

Given a generator G , we investigate the optimal discriminator D as follows.

Lemma 1. *For a fixed generator g_θ in the MIM-based GAN, the optimal discriminator D is obtained as*

$$D_{\text{MIM}}^*(\mathbf{x}) = \frac{1}{2} + \frac{1}{2} \ln \frac{P(\mathbf{x})}{P_{g_\theta}(\mathbf{x})}, \quad (5)$$

where P and P_{g_θ} are densities of the distributions \mathbb{P} and \mathbb{P}_{g_θ} .

Proof. Considering the training criterion of discriminator D (with a given generator g_θ), we just minimize

$$L_{\text{MIM}}(D, G) = \int_{\mathbf{x}} [P(\mathbf{x}) \exp(1 - D(\mathbf{x})) + P_{g_\theta}(\mathbf{x}) \exp(D(\mathbf{x}))] d\mathbf{x}, \quad (6)$$

and the corresponding solution is the optimal D .

As for a function $f(u) = a \exp(1 - u) + b \exp(u)$ ($a > 0, b > 0$), we have the solution $u = \frac{1}{2} + \ln(\frac{a}{b})$ achieving $\frac{\partial f(u)}{\partial u} = -a \exp(1 - u) + b \exp(u) = 0$. Besides, due to the fact that the second order derivative

$\frac{\partial^2 f(u)}{\partial u^2} = a \exp(1-u) + b \exp(u) > 0$, implying the convexity of $f(u)$, the solution $u = \frac{1}{2} + \ln(\frac{a}{b})$ is obtained, which achieves the minimum of $f(u)$. Then, it is easy to verify this Lemma. \square

By substituting D_{MIM}^* into $L_{\text{MIM}}(D, G)$, it is not difficult to have

$$\begin{aligned} L_{\text{MIM}}(D = D_{\text{MIM}}^*, G) &= \mathbb{E}_{\mathbf{x} \sim \mathbb{P}}[\exp(1 - D_{\text{MIM}}^*(\mathbf{x}))] + \mathbb{E}_{\mathbf{x} \sim \mathbb{P}_{g_\theta}}[\exp(D_{\text{MIM}}^*(\mathbf{x}))] \\ &= \mathbb{E}_{\mathbf{x} \sim \mathbb{P}} \left[\exp \left(\frac{1}{2} + \ln \left(\frac{P(\mathbf{x})}{P_{g_\theta}(\mathbf{x})} \right)^{-\frac{1}{2}} \right) \right] + \mathbb{E}_{\mathbf{x} \sim \mathbb{P}_{g_\theta}} \left[\exp \left(\frac{1}{2} + \ln \left(\frac{P(\mathbf{x})}{P_{g_\theta}(\mathbf{x})} \right)^{\frac{1}{2}} \right) \right] \\ &= \sqrt{e} \left\{ \mathbb{E}_{\mathbf{x} \sim \mathbb{P}} \left[\left(\frac{P(\mathbf{x})}{P_{g_\theta}(\mathbf{x})} \right)^{-\frac{1}{2}} \right] + \mathbb{E}_{\mathbf{x} \sim \mathbb{P}_{g_\theta}} \left[\left(\frac{P_{g_\theta}(\mathbf{x})}{P(\mathbf{x})} \right)^{-\frac{1}{2}} \right] \right\}. \end{aligned} \quad (7)$$

Proposition 1. *As for the MIM-based GAN, the optimal solution of equivalent objective function with the optimal discriminator, i.e. $L_{\text{MIM}}(D = D_{\text{MIM}}^*, G)$ (mentioned in Eq. (7)), is achieved if and only if $\mathbb{P} = \mathbb{P}_{g_\theta}$, where $L_{\text{MIM}}(D = D_{\text{MIM}}^*, G)$ reaches $2\sqrt{e}$.*

Proof. In the case $\mathbb{P} = \mathbb{P}_{g_\theta}$ (implying $D_{\text{MIM}}^*(\mathbf{x}) = \frac{1}{2}$), we have the value of Eq. (7) as $L_{\text{MIM}}(D = \frac{1}{2}, G) = \sqrt{e}(1+1) = 2\sqrt{e}$. This is the maximum value of $L_{\text{MIM}}(D = D_{\text{MIM}}^*, G)$, reached at the point $\mathbb{P} = \mathbb{P}_{g_\theta}$.

According to the expression of Eq. (7), we have the equivalent formulation as follows

$$\begin{aligned} \max_{g_\theta} L_{\text{MIM}}(D = D_{\text{MIM}}^*, G) &\Leftrightarrow \max_{g_\theta} \sqrt{e} \left\{ \ln \mathbb{E}_{\mathbf{x} \sim \mathbb{P}} \left[\left(\frac{P(\mathbf{x})}{P_{g_\theta}(\mathbf{x})} \right)^{-\frac{1}{2}} \right] + \ln \mathbb{E}_{\mathbf{x} \sim \mathbb{P}_{g_\theta}} \left[\left(\frac{P_{g_\theta}(\mathbf{x})}{P(\mathbf{x})} \right)^{-\frac{1}{2}} \right] \right\}. \end{aligned} \quad (8)$$

Then, it is not difficult to see that

$$\max_{g_\theta} L_{\text{MIM}}(D = D_{\text{MIM}}^*, G) \Leftrightarrow \min_{g_\theta} \frac{\sqrt{e}}{2} \left\{ R_{\alpha=\frac{1}{2}}(\mathbb{P} || \mathbb{P}_{g_\theta}) + R_{\alpha=\frac{1}{2}}(\mathbb{P}_{g_\theta} || \mathbb{P}) \right\}, \quad (9)$$

where $R_{\alpha=\frac{1}{2}}(\cdot)$ is the Renyi divergence (whose parameter satisfies $\alpha = \frac{1}{2}$) which is defined as

$$R_\alpha(\mathbb{P} || \mathbb{Q}) = \frac{1}{\alpha - 1} \ln \left\{ \mathbb{E}_{\mathbf{x} \sim \mathbb{P}} \left[\left(\frac{P(\mathbf{x})}{Q(\mathbf{x})} \right)^{\alpha-1} \right] \right\}, \quad (\alpha > 0, \alpha \neq 1). \quad (10)$$

Due to the fact that Renyi divergence (with parameter $\alpha = \frac{1}{2}$) reaches the minimum when $\mathbb{P} = \mathbb{Q}$, it is readily seen that $2\sqrt{e}$ is the maximum value of $L_{\text{MIM}}(D = D_{\text{MIM}}^*, G)$ and the corresponding solution is $\mathbb{P} = \mathbb{P}_{g_\theta}$, that is to say, the real data is replicated. \square

Remark 1. *Similar to the original GAN, there exists a training equilibrium for the two-player optimization game in the MIM-based GAN. In this regard, the global optimality lies at the point of $\mathbb{P} = \mathbb{P}_{g_\theta}$. However, due to the different expressions of optimization game, the training process (to the equilibrium point) for the MIM-based GAN is not the same as that for the original GAN, which is revealed by Eq. (5) and Eq. (7). Therefore, the differences between the two GANs may bring some novelties in theory and applications.*

2) *Gradient of generator under the optimal discriminator:*

With regard to analyze the training process of GANs, it is worth investigating the gradient of objective function. Here, we would like to discuss the gradient of generator in the case of the optimal discriminator, due to the fact that if the equilibrium is approximated, the discriminator is trained well already.

Proposition 2. *As for the MIM-based GAN, let $g_\theta : \mathcal{Z} \rightarrow \mathcal{X}$ be a differentiable function to generate data. If there exists the optimal discriminator $D_{MIM}^*(\mathbf{x}) = \frac{1}{2} + \frac{1}{2} \ln \frac{P(\mathbf{x})}{P_{g_\theta}(\mathbf{x})}$, the gradient with respect to the parameter θ in the corresponding generator, is given by*

$$\begin{aligned}
& \nabla_{\theta} \mathbb{E}_{\mathbf{z} \sim \mathbb{P}_z} [\exp(D_{MIM}^*(g_\theta(\mathbf{z})))] \\
&= \mathbb{E}_{\mathbf{z} \sim \mathbb{P}_z} \left[\nabla_{\theta} \exp \left(\frac{1}{2} + \frac{1}{2} \ln \left(\frac{P(g_\theta(\mathbf{z}))}{P_{g_\theta}(g_\theta(\mathbf{z}))} \right) \right) \right] \\
&= \sqrt{e} \mathbb{E}_{\mathbf{z} \sim \mathbb{P}_z} \left[\nabla_{\theta} \left(\frac{P(g_\theta(\mathbf{z}))}{P_{g_\theta}(g_\theta(\mathbf{z}))} \right)^{\frac{1}{2}} \right] \\
&= \frac{\sqrt{e}}{2} \mathbb{E}_{\mathbf{z} \sim \mathbb{P}_z} \left[\left(\frac{P(g_\theta(\mathbf{z}))}{P_{g_\theta}(g_\theta(\mathbf{z}))} \right)^{-\frac{1}{2}} \frac{\nabla_{\theta} P(g_\theta(\mathbf{z})) P_{g_\theta}(g_\theta(\mathbf{z})) - \nabla_{\theta} P_{g_\theta}(g_\theta(\mathbf{z})) P(g_\theta(\mathbf{z}))}{P_{g_\theta}^2(g_\theta(\mathbf{z}))} \right] \quad (11) \\
&= \frac{\sqrt{e}}{2} \mathbb{E}_{\mathbf{z} \sim \mathbb{P}_z} \left[\frac{\nabla_{\theta} P(g_\theta(\mathbf{z})) \sqrt{\frac{P_{g_\theta}(g_\theta(\mathbf{z}))}{P(g_\theta(\mathbf{z}))}} - \nabla_{\theta} P_{g_\theta}(g_\theta(\mathbf{z})) \sqrt{\frac{P(g_\theta(\mathbf{z}))}{P_{g_\theta}(g_\theta(\mathbf{z}))}}}{P_{g_\theta}(g_\theta(\mathbf{z}))} \right].
\end{aligned}$$

Remark 2. *As for the gradient of generator under the optimal discriminator, it is not difficult to see if the generative distribution is approaching to the real distribution, the gradient is getting small. In other words, if the training equilibrium is reached closely, the end of training state will be achieved.*

3) *Anti-interference ability of generator:*

Consider the fact that the discriminator makes a difference on the generator during the adversarial training process of GANs. Specifically, when there exists a disturbance in the discriminator, the generator will be drawn into the unstable training in some degree. Consequently, it is required to analyze the anti-interference ability of generator with respect to the disturbance in the discriminator.

Proposition 3. *Let $g_\theta : \mathcal{Z} \rightarrow \mathcal{X}$ be a differentiable function to generate the data denoted by $g_\theta(\mathbf{z})$, whose distribution is denoted by \mathbb{P}_{g_θ} corresponding to the real distribution \mathbb{P} . Let \mathbb{P}_z be the distribution for \mathbf{z} as well as D be a discriminator ($D \in [0, 1]$). Consider the stability for the gradient of generator in the MIM-based GAN in the two following cases.*

• Assuming $D - \tilde{D}^* = \epsilon$ (ϵ denotes a small disturbance which satisfies $\epsilon \in [0, 1]$, as well as \tilde{D}^* is the ideal perfect discriminator i.e. $\tilde{D}^*(g_\theta(\mathbf{z})) = 0$), we have

$$\begin{aligned} \nabla_{\theta} \mathbb{E}_{\mathbf{z} \sim \mathbb{P}_z} [\exp(D(g_\theta(\mathbf{z})))] &= \mathbb{E}_{\mathbf{z} \sim \mathbb{P}_z} [\exp(D(g_\theta(\mathbf{z}))) \nabla_{\mathbf{x}} D(\mathbf{x}) \nabla_{\theta} g_{\theta}(\mathbf{z})] \\ &= \mathbb{E}_{\mathbf{z} \sim \mathbb{P}_z} [\exp(\tilde{D}^*(g_\theta(\mathbf{z})) + \epsilon) \nabla_{\mathbf{x}} D(\mathbf{x}) \nabla_{\theta} g_{\theta}(\mathbf{z})] \\ &= \exp(\epsilon) \mathbb{E}_{\mathbf{z} \sim \mathbb{P}_z} [\nabla_{\mathbf{x}} D(\mathbf{x}) \nabla_{\theta} g_{\theta}(\mathbf{z})]. \end{aligned} \quad (12)$$

• Assuming $D - \check{D}^* = \epsilon$ (ϵ is a small disturbance which satisfies $|\epsilon| < \frac{1}{2}$, as well as \check{D}^* is the worst discriminator i.e. $\check{D}^*(g_\theta(\mathbf{z})) = \frac{1}{2}$ implying that the training equilibrium is achieved), we have

$$\begin{aligned} \nabla_{\theta} \mathbb{E}_{\mathbf{z} \sim \mathbb{P}_z} [\exp(D(g_\theta(\mathbf{z})))] &= \mathbb{E}_{\mathbf{z} \sim \mathbb{P}_z} [\exp(\check{D}^*(g_\theta(\mathbf{z})) + \epsilon) \nabla_{\mathbf{x}} D(\mathbf{x}) \nabla_{\theta} g_{\theta}(\mathbf{z})] \\ &= \exp\left(\frac{1}{2} + \epsilon\right) \mathbb{E}_{\mathbf{z} \sim \mathbb{P}_z} [\nabla_{\mathbf{x}} D(\mathbf{x}) \nabla_{\theta} g_{\theta}(\mathbf{z})]. \end{aligned} \quad (13)$$

Corollary 1. Let $g_\theta : \mathcal{Z} \rightarrow \mathcal{X}$ be a differentiable function that is used to generate data following the distribution \mathbb{P}_{g_θ} . Let \mathbb{P}_z be the distribution for \mathbf{z} ($\mathbf{z} \in \mathcal{Z}$), \mathbb{P} be the real data distribution, and D be a discriminator ($D \in [0, 1]$). Consider the condition satisfying $D - \tilde{D}^* = \epsilon$ ($\epsilon \in [0, 1]$ and $\tilde{D}^*(g_\theta(\mathbf{z})) = 0$ denoting the ideal perfect discriminator) or $D - \check{D}^* = \epsilon$ ($|\epsilon| < \frac{1}{2}$ and $\check{D}^*(g_\theta(\mathbf{z})) = \frac{1}{2}$ denoting the worst discriminator). In this regard, the gradient of generator in the MIM-based GAN has more anti-interference ability of generator than that in the original GAN.

Proof. Please see the Appendix A. □

Remark 3. From the perspective of the gradient of generator, the disturbance in the discriminator is taken into a function to provide a multiplicative parameter for the gradient. In fact, the different gradients in the original GAN and MIM-based GAN are resulted from the different objective functions. Particularly, the exponential function in the gradient of MIM-based GAN is originated from the the partial derivative of its objective function with exponential one. While, the reciprocal function in the gradient of original GAN is derived from the logarithmic function of the objective function.

III. RARE EVENTS ANALYSIS IN GANS

From a new viewpoint to analyze GANs, we focus on the case that real data contains rare events and investigate how rare events make differences on the data generation and the corresponding applications of GANs.

A. Effect of rare events on generator

With respect to the training process of GANs, we usually train a pretty good discriminator and use it to lead the generator to reach its optimal objective function. Then, a better generator is also obtained to train the discriminator as a feedback. This process runs iteratively until reaches the equilibrium point. In this regard, if we have an optimal discriminator (an ideal case), our goal is to maximize the objective function by selecting an appropriate generator (according to Eq. (7)). In this case, relatively fewer occurrence events make less effects on the objective function. It is implied that the generator ignores smaller probability events (usually regarded as rare events) in some degree by maximizing the major part of objective function. As a result, it is necessary to discuss the proportion of rare events in the objective functions of generators. Before this, we shall introduce a kind of rare events characterization to provide a specific example for rare events processing.

In general, rare events and large probability ones can be regarded to belong to two different classes, which implies there exists a binary distribution $\{P(\bar{\Theta}), P(\Theta)\}$ where $P(\bar{\Theta}) = p$ ($p \ll \frac{1}{2}$) and $P(\Theta) = 1 - p$ ($\bar{\Theta}$ denotes the rare events and Θ denotes the normal ones). For instance, the minority set and majority set match this case in statistics. Specifically, we have the two sets satisfying

$$\begin{cases} \bar{\Theta} = \left\{ m_k \mid \left| \frac{m_k}{M} - p_k \right| \geq \xi, k = 1, 2, \dots, K \right\}, \\ \Theta = \left\{ m_k \mid \left| \frac{m_k}{M} - p_k \right| < \xi, k = 1, 2, \dots, K \right\}, \end{cases} \quad (14)$$

and the corresponding probability elements given by

$$\begin{cases} P\{\bar{\Theta}\} \leq K \max_k P\left\{ \left| \frac{m_k}{M} - p_k \right| \geq \xi \right\} \leq \delta, \\ P\{\Theta\} = 1 - P\{\bar{\Theta}\} > 1 - \delta, \end{cases} \quad (15)$$

which results from the weak law of large numbers $P\left\{ \left| \frac{m_k}{M} - p_k \right| < \xi \right\} > 1 - \delta$, where m_k is the occurrence number of a_k (the sample support space is $\{a_1, a_2, \dots, a_K\}$), p_k denotes a probability element from a distribution $\{p, p_2, \dots, p_K\}$, M is the sample number, as well as $0 < \xi \ll 1$ and $0 < \delta \ll 1$.

Based on the above discussion, we investigate how much proportion of rare events will be taken in the objective functions of GANs. This may reflect the rare events generation for the generator of GANs.

Proposition 4. *Let \mathbb{P} be the real data distribution involved with rare events, which is given by $\mathbb{P} = \{p, 1-p\}$ ($0 < p \ll \frac{1}{2}$) corresponding to the Eq. (15). Let $g_\theta : \mathcal{Z} \rightarrow \mathcal{X}$ be a differentiable function for the generative data which follows the distribution \mathbb{P}_{g_θ} where $\mathbb{P}_{g_\theta} = \{p + \varepsilon p^\gamma, 1 - p - \varepsilon p^\gamma\} = \{q, 1 - q\}$ ($q < \frac{1}{2}$). Consider the case that the optimal discriminator is achieved, which implies $D_{\text{MIM}}^*(\mathbf{x}) = \frac{1}{2} + \frac{1}{2} \ln \frac{P(\mathbf{x})}{P_{g_\theta}(\mathbf{x})}$ for the*

MIM-based GAN. In this case, the proportion of rare events in the objective function of generator is given by

$$\Upsilon_{MIM} \approx \frac{\frac{p+q}{2} - \frac{1}{8}\varepsilon^2 p^{2\gamma-1}}{1 - \frac{1}{8}\varepsilon^2 \frac{p^{2\gamma-1}}{1-p}}, \quad (16)$$

where ε and γ denote a small disturbance parameter and an adjustable parameter (regarded as a constant) respectively.

Proof. In the light of the condition $\mathbb{P}_{g_\theta} = \{p + \varepsilon p^\gamma, 1 - p - \varepsilon p^\gamma\} = \{q, 1 - q\}$ ($q < \frac{1}{2}$), it is known that ε and γ represent the deviation between the two distributions \mathbb{P} and \mathbb{P}_{g_θ} . Considering the optimal discriminator in the MIM-based GAN and the Eq. (7), it is readily seen that

$$\begin{aligned} L_{MIM}(D = D_{MIM}^*, G) &= \sqrt{e} \left\{ \mathbb{E}_{\mathbf{x} \sim \mathbb{P}} \left[\left(\frac{P(\mathbf{x})}{P_{g_\theta}(\mathbf{x})} \right)^{-\frac{1}{2}} \right] + \mathbb{E}_{\mathbf{x} \sim \mathbb{P}_{g_\theta}} \left[\left(\frac{P_{g_\theta}(\mathbf{x})}{P(\mathbf{x})} \right)^{-\frac{1}{2}} \right] \right\} \\ &= 2\sqrt{e} \left\{ p(1 + \varepsilon p^{\gamma-1})^{\frac{1}{2}} + (1-p) \left(1 - \frac{\varepsilon p^\gamma}{1-p} \right)^{\frac{1}{2}} \right\}. \end{aligned} \quad (17)$$

Focusing on the rare events reflected into the probability element p rather than $(1-p)$ ($0 < p \ll \frac{1}{2}$), we have the proportion of rare events in the $L_{MIM}(D = D_{MIM}^*, G)$ as follows

$$\begin{aligned} \Upsilon_{MIM} &= \frac{2\sqrt{e} \left\{ p(1 + \varepsilon p^{\gamma-1})^{\frac{1}{2}} \right\}}{L_{MIM}(D = D_{MIM}^*, G)} \\ &\stackrel{(a)}{=} \frac{p + \frac{1}{2}\varepsilon p^\gamma - \frac{1}{8}\varepsilon^2 p^{2\gamma-1} + o(\varepsilon^2)}{\left\{ p + \frac{1}{2}\varepsilon p^\gamma - \frac{1}{8}\varepsilon^2 p^{2\gamma-1} + o(\varepsilon^2) \right\} + \left\{ (1-p) - \frac{1}{2}\varepsilon p^\gamma - \frac{1}{8}\varepsilon^2 \frac{p^{2\gamma}}{1-p} + o(\varepsilon^2) \right\}} \\ &= \frac{\frac{p+q}{2} - \frac{1}{8}\varepsilon^2 p^{2\gamma-1} + o(\varepsilon^2)}{1 - \frac{1}{8}\varepsilon^2 \frac{p^{2\gamma-1}}{1-p} + o(\varepsilon^2)} \\ &\approx \frac{\frac{p+q}{2} - \frac{1}{8}\varepsilon^2 p^{2\gamma-1}}{1 - \frac{1}{8}\varepsilon^2 \frac{p^{2\gamma-1}}{1-p}}, \end{aligned} \quad (18)$$

where the equality (a) is derived from Taylor's theorem. \square

Corollary 2. Let \mathbb{P} and \mathbb{P}_{g_θ} be the real distribution and the generative one, where $\mathbb{P} = \{p, 1 - p\}$ ($0 < p \ll \frac{1}{2}$) and $\mathbb{P}_{g_\theta} = \{p + \varepsilon p^\gamma, 1 - p - \varepsilon p^\gamma\} = \{q, 1 - q\}$ ($q < \frac{1}{2}$). Consider the case that the optimal discriminator is achieved, which implies $D_{MIM}^*(\mathbf{x}) = \frac{1}{2} + \frac{1}{2} \ln \frac{P(\mathbf{x})}{P_{g_\theta}(\mathbf{x})}$ for the MIM-based GAN and $D_{KL}^*(\mathbf{x}) = \frac{P(\mathbf{x})}{P(\mathbf{x}) + P_{g_\theta}(\mathbf{x})}$ for the original GAN. In this regard, compared with the original GAN, the MIM-based GAN usually maintains higher proportion of rare events in the objective function of generator, namely $\Upsilon_{MIM} \geq \Upsilon_{KL}$, where the equality is hold in the case $p = q$.

Proof. Similar to Proposition 4, it is readily seen that

$$\begin{aligned}
& L_{\text{KL}}(D = D_{\text{KL}}^*, G) \\
&= \mathbb{E}_{\mathbf{x} \sim \mathbb{P}} \left[\ln \frac{P(\mathbf{x})}{P(\mathbf{x}) + P_{g_\theta}(\mathbf{x})} \right] + \mathbb{E}_{\mathbf{x} \sim \mathbb{P}_{g_\theta}} \left[\ln \frac{P_{g_\theta}(\mathbf{x})}{P(\mathbf{x}) + P_{g_\theta}(\mathbf{x})} \right] \\
&= -p \ln(2 + \varepsilon p^{\gamma-1}) - (1-p) \ln\left(2 - \varepsilon \frac{p^\gamma}{1-p}\right) \\
&\quad + p(1 + \varepsilon p^{\gamma-1}) \ln\left(1 - \frac{1}{2 + \varepsilon p^{\gamma-1}}\right) + (1-p - \varepsilon p^\gamma) \ln\left(1 - \frac{1}{2 - \varepsilon \frac{p^\gamma}{1-p}}\right),
\end{aligned} \tag{19}$$

in which the the proportion of rare events is given by

$$\begin{aligned}
\Upsilon_{\text{KL}} &= \frac{-p \ln(2 + \varepsilon p^{\gamma-1}) + p(1 + \varepsilon p^{\gamma-1}) \ln\left(1 - \frac{1}{2 + \varepsilon p^{\gamma-1}}\right)}{L_{\text{KL}}(D = D_{\text{KL}}^*, G)} \\
&= \frac{\frac{p+q}{2} - \frac{1}{8 \ln 2} \varepsilon^2 p^{2\gamma-1} + o(\varepsilon^2)}{1 - \frac{1}{8 \ln 2} \varepsilon^2 \frac{p^{2\gamma-1}}{1-p} + o(\varepsilon^2)} \\
&\approx \frac{\frac{p+q}{2} - \frac{1}{8 \ln 2} \varepsilon^2 p^{2\gamma-1}}{1 - \frac{1}{8 \ln 2} \varepsilon^2 \frac{p^{2\gamma-1}}{1-p}}.
\end{aligned} \tag{20}$$

According to $p < \frac{1}{2}$ and $q < \frac{1}{2}$, we have $\frac{p+q}{2(1-p)} < 1$. Then, it is not difficult to see that the term of right-hand side in Eq. (18) is larger than that in Eq. (20), which verifies the proposition. \square

Remark 4. Consider that the objective function guides the generator networks of GANs to generate fraudulent fake data. Since the dominant component of objective function depends on larger probability events, a generator prefers to output the data belonging to the normal data set. In order to reveal the ability of rare events generation for generators, it is significant to compare the rare events proportion in different objective functions, which is discussed in Proposition 4 and Corollary 2. Furthermore, according to Proposition 3 and Corollary 1, it is implied that when there exists some disturbance for rare events, the MIM-based GAN still keeps more stable than the original GAN, which means the former has more anti-interference ability to generate rare events. To sum up, it is reasonable that the MIM-based GAN performs more efficient than the original GAN on rare events generation.

B. GAN-based anomaly detection

As a promising application of GANs, anomaly detection has attracted much attention of researchers. According to the principle of GANs, it is known that by resorting to the Nash equilibrium of objective function rather than a single optimization, the generator gains more representative power and specificity to represent the real data. Actually, to identify anomalies (belonging to rare events) with GANs, the outputs of generator network are regarded to approximate normal events. Then, by use of identification tools such

as Euclidean distance, anomalies are detected due to their evident differences from the generative events (corresponding to normal ones). Simultaneously, a trained discriminator network is also used to dig out the anomalies not in the generative data.

Due to the similar principle between the original GAN and MIM-based GAN, the anomaly detection method is not only suitable for the former but also for the latter. In this regard, we will introduce how to build a data processing model based on GANs (such as the original GAN and the MIM-based GAN), and how to use it to identify anomalous events (hardly ever appearing in the training data) in details.

1) Procedure for anomaly detection with GANs:

We shall introduce a procedure of GAN-based detection, which provides a general framework for GANs to detect anomalies (where we take the MIM-based GAN as an example). As for our goal, it is to allocate labels $\{0, 1\}$ (“0” for normal events and “1” for anomalous ones) to testing samples. The procedure is described as follows.

- **Step 1: data processing preparation with GANs**

At first, we generate some fake data similar to the real data by use of GAN. By feeding training data x and the random data z in the latent space to the MIM-based GAN model, we train the generator and discriminator (both based on neural networks) with the two-player maxmin game given by Eq. (4) to generate the imitative data.

- **Step 2: anomaly score computing**

In this step, a detection measurement tool named anomaly score is designed based on the generative data and the corresponding GANs. We trained the discriminator D and generator G for enough iterations and then make use of them to identify the anomalous events by means of the anomaly score which is introduced in Section III-B2.

- **Step 3: decision for detection**

By using anomaly scores of the testing samples (obtained in the step 2) to make a decision for detection, we label each sample in the testing dataset as

$$A^{\text{test}} = \begin{cases} 1, & \text{for } S^{\text{test}} > \Gamma, \\ 0, & \text{otherwise,} \end{cases} \quad (21)$$

where A^{test} is a label for a testing sample, whose non-zero value indicates a detected rare event, i.e. the anomaly score is higher than a predefined threshold Γ .

2) Anomaly score based on both discriminator and generator:

The superiority of architecture of GANs is that we jointly train two neural networks, namely the discriminator and the generator, which makes one more decision tool available. We would like to exploit both discriminator and generator as tools to dig out anomalies. In fact, there are two parts in the GAN-based anomaly detection as follows.

- **Generator-based anomaly detection**

In terms of the trained generator G which generates realistic samples, it is regarded as a mapping from a latent data space to the real data space, namely $G : \mathcal{Z} \rightarrow \mathcal{X}$. Since that it is more likely to learn the normal data which occurs frequently, the generator tends to reflect the principal components of the real data' distribution. In this regard, the generator is also considered as an inexplicit model to reflect the normal events. Considering the smooth transitions in the latent space, we have the similar outputs of generator when the inputs are close enough in the latent space. Furthermore, if we can find the latent data z which is the most likely mapped into the testing data x , the similarity between testing data x and reconstructed testing data $G(z)$ reveals how much extent x can be viewed as a sample drawn from the distribution reflected by G . As a result, it is applicable to use the residuals between x and $G(z)$ to identify the anomalous events hidden in testing data. In addition, we should also consider the discriminator loss as a regularization for the residual loss, which ensures the reconstructed data $G(z)$ to lie on the manifold \mathcal{X} .

- **Discriminator-based anomaly detection**

The trained discriminator D which distinguishes generative data from real data with high sensitivity, is a direct tool to detect the anomalies.

Considering GAN-based anomaly detection, it is the most important to find the optimal z in the latent space, which is mapped to the testing samples approximately. In this regard, a random z from the latent space is chosen and put into the generator to produce the reconstructed sample $G(z)$ which corresponds to the sample x . Then, we update z in the latent space by means of gradient descent with respect to the loss function given by Eq. (23). After sufficient iteration (namely the loss function hardly ever decreasing), we gain the most likely latent data z mapped into the testing data, which means the optimal z_{opt} is obtained by

$$z_{\text{opt}} = \arg \min_z J_{\text{error}}(\mathbf{x}, z), \quad (22)$$

where the loss function $J_{\text{error}}(\mathbf{x}, z)$ is given by

$$J_{\text{error}}(\mathbf{x}, z) = (1 - \lambda) \|\mathbf{x} - G(z)\|_p + \lambda H_{\text{ce}}(D(G(z)), \beta), \quad (23)$$

in which λ is an adjustable weight ($0 < \lambda < 1$), $\|\cdot\|_p$ is the p -norm (usually $p = 2$), and $H_{ce}(\cdot, \cdot)$ denotes the sigmoid cross entropy which is given by

$$H_{ce}(D(G(\mathbf{z})), \beta) = -\beta \ln \left[\frac{1}{1 + \exp(-D(G(\mathbf{z})))} \right] - (1 - \beta) \ln \left[1 - \frac{1}{1 + \exp(-D(G(\mathbf{z})))} \right], \quad (24)$$

with the target $\beta = 1$.

Furthermore, by combining the $J_{\text{error}}(\mathbf{x}, \mathbf{z})$ and $D(\mathbf{x})$, we have the anomaly detection loss, referred to as *anomaly score*, which is given by

$$S^{\text{test}} = (1 - \eta) J_{\text{error}}(\mathbf{x}, \mathbf{z}_{\text{opt}}) + \eta H_{ce}(D(\mathbf{x}), \beta), \quad (25)$$

where the adjustable weight satisfies $0 < \eta < 1$, as well as, $\beta = 1$.

In view of the above descriptions, the outputs of trained discriminator and generator are exploited to calculate a set of anomaly scores for test data. Then, we detect the anomalies by use of the decision-making tool described as Eq. (21).

3) Analysis for the anomaly detection with GANs:

Here, we shall discuss the intrinsic principle of the above anomaly detection method. Specifically, we take the detection method with the MIM-based GAN as an example to give some analyses. Considering that the anomaly score (as a main part in the detection method) consists of two parts related to GANs, we will analyze the corresponding two parts, respectively, as follows.

- **Analysis for generator-based detection:** As for the generator G which maps the latent samples into realistic samples, it tends to generate the data with large probability in the real data set. Assume the real data are classified into two sets according to their probability, namely the large probability events set Ω_{large} and the small probability events (or rare events) set Ω_{rare} . In this case, we have the proportion of large probability events in the objective function mentioned in Eq. (3) as follows

$$\begin{aligned} R_{\Omega_{\text{large}}} &= \frac{\int_{\Omega_{\text{large}}} [P(\mathbf{x}) \exp(1 - D(\mathbf{x})) + P_{g_\theta}(\mathbf{x}) \exp(D(\mathbf{x}))] d\mathbf{x}}{\int_{\Omega_{\text{large}} + \Omega_{\text{rare}}} [P(\mathbf{x}) \exp(1 - D(\mathbf{x})) + P_{g_\theta}(\mathbf{x}) \exp(D(\mathbf{x}))] d\mathbf{x}} \\ &\stackrel{(b)}{=} \frac{\int_{\Omega_{\text{large}}} \left[P(\mathbf{x}) \left(\frac{P(\mathbf{x})}{P_{g_\theta}(\mathbf{x})} \right)^{-\frac{1}{2}} + P_{g_\theta}(\mathbf{x}) \left(\frac{P_{g_\theta}(\mathbf{x})}{P(\mathbf{x})} \right)^{-\frac{1}{2}} \right] d\mathbf{x}}{\int_{\Omega_{\text{large}} + \Omega_{\text{rare}}} \left[P(\mathbf{x}) \left(\frac{P(\mathbf{x})}{P_{g_\theta}(\mathbf{x})} \right)^{-\frac{1}{2}} + P_{g_\theta}(\mathbf{x}) \left(\frac{P_{g_\theta}(\mathbf{x})}{P(\mathbf{x})} \right)^{-\frac{1}{2}} \right] d\mathbf{x}} \\ &= \frac{\int_{\Omega_{\text{large}}} [P(\mathbf{x}) P_{g_\theta}(\mathbf{x})]^{\frac{1}{2}} d\mathbf{x}}{\int_{\Omega_{\text{large}} + \Omega_{\text{rare}}} [P(\mathbf{x}) P_{g_\theta}(\mathbf{x})]^{\frac{1}{2}} d\mathbf{x}}, \end{aligned} \quad (26)$$

where the equality (b) is obtained by replacing the discriminator D with D_{MIM}^* (in Eq. (5)). When the generative probability $P_{g_\theta}(\mathbf{x})$ is close to the real probability $P(\mathbf{x})$, we have $P_{g_\theta}(\mathbf{x}) \approx P(\mathbf{x}) \gg 0$ in the region $\{\mathbf{x} \in \Omega_{\text{large}}\}$, while in the region $\{\mathbf{x} \in \Omega_{\text{rare}}\}$, $P_{g_\theta}(\mathbf{x})$ is pretty small or even approximates to zero. Then, the large probability events proportion in the objective function is close to the corresponding probability, that is, $R_{\Omega_{\text{large}}} \approx \frac{\int_{\Omega_{\text{large}}} P(\mathbf{x}) d\mathbf{x}}{\int_{\Omega_{\text{large}} + \Omega_{\text{rare}}} P(\mathbf{x}) d\mathbf{x}} = \int_{\Omega_{\text{large}}} P(\mathbf{x}) d\mathbf{x} \rightarrow 1$. This implies that the generative data $G(\mathbf{z})$ is more likely to belong to the large probability events set (that is usually the principle component of normal events), regarded as the whole of normal events. It is readily seen that large probability events make more effects on training the generator than rare events with small probability (which usually consists of the small part of normal events and anomalous ones). Furthermore, in the loss function $J_{\text{error}}(\mathbf{x}, \mathbf{z})$, $\|\mathbf{x} - G(\mathbf{z})\|_p$ is minimized to let \mathbf{x} be close to a generative event (regarded as a normal event), while $H_{\text{ce}}(D(G(\mathbf{z})), \beta)$ enforces $G(\mathbf{z})$ to be in the real data space. As a result, large enough $J_{\text{error}}(\mathbf{x}, \mathbf{z})$ usually reflect the anomalous events, which plays an important role in the anomaly score.

- **Analysis for discriminator-based detection:** As the second term of anomaly score, $H_{\text{ce}}(D(\mathbf{x}), \beta)$ is based on a well trained discriminator (similar to the optimal one). In terms of the ideal discriminator as Eq. (5), it can make a decision whether a sample belongs to the training data set (namely the real data set) or not. In particular, when a testing data does not appear in the training data set, the corresponding value of $D(\mathbf{x})$ approximates to zero (which implies a large cross entropy). While, the values of $D(\mathbf{x})$ for other testing data (included in the training data set) are more likely close to $\frac{1}{2}$. In this regard, the discriminator is exploited for anomaly detection.

Remark 5. *It is necessary to give comparisons for the original GAN and MIM-based GAN to detect anomalies. Due to the similar two-player game principle, the original GAN and MIM-based GAN have analogous characteristics in the anomaly detection. However, from the discussion of Corollary 2, we know that the MIM-based GAN pays more attention to the small part of normal events (which are with smaller probability) in some degree than the original GAN. In other words, the smaller probability events in the normal events set are more likely generated rather than lost, which indicates that the regarded anomalous events set is more close to the real anomalous events set and contains less normal events with small probability. This has a positive impact on the anomaly detection.*

IV. EXPERIMENTS

Now, we present experimental results to show the efficiency of MIM-based GAN and other classical GANs. Particularly, we compare our method with other adversarial networks (such as the original GAN, LSGAN and WGAN) with respect to data generation and anomaly detection. Our main findings for the MIM-based GAN may be that:

- Compared with some classical GANs, training performance improvements are available during the training process to the equilibrium;
- By use of MIM-based GAN, there exists the better performance on detecting anomalies than other classical GANs.

A. Datasets

As for the datasets, artificial data and real data are considered to compare different approaches and evaluate their performance. Particularly, on one hand, we take artificial Gaussian distribution data as an example, whose mean and standard deviation are denoted by μ and σ respectively. The Gaussian distribution $\mathcal{N}(\mu, \sigma)$ is chosen as $\mathcal{N}(\mu = 4, \sigma = 1.25)$ in our experiments. On the other hand, several real datasets (including the MNIST dataset and Outlier Detection DataSet (ODDS)) are collected online, whose details are listed as follows.

- **MNIST**: As for this dataset, 10 different classes of digits $\{0, 1, 2, \dots, 9\}$ in MNIST are generated by use of GANs. In order to apply this case into anomaly detection, we choose one kind of digit class (such as “0”) as the rare events (namely anomalies), while the rest parts are treated as normal ones. In other words, there exist 10% rare events mixed in the whole dataset. The training set consists of 60,000 image samples (28×28 pixel gray handwritten digital images), while there are 10,000 image samples in the testing set.
- **ODDS**: Considering that it is necessary to process real-world datasets in practice, we shall investigate several anomaly detection datasets from the ODDS repository as follows.
 - Cardiotocography*: The Cardiotocography dataset in ODDS repository has 21 features in each sample, such as Fetal Heart Rate (FHR) and Uterine Contraction (UC) features. There are 1,831 samples in this dataset, including 176 samples (9.6% data) that belong to the pathologic class, namely the anomalous events class.

b) Thyroid: The Thyroid dataset contains 6 real attributes (namely data dimension). In this database, there are 3,772 samples, containing 93 hyperfunction samples (2.5% data) which belong to the anomalous events class.

c) Musk: The Musk dataset in ODDS repository consists of 3,062 samples including 3.2% anomalies. Specifically, the dataset contains several-musks and non-musk classes, which are regarded as the inliers and outliers (or anomalies) respectively. By the way, there exist 166 features in each sample.

B. Experiment details

1) Training performance experiments:

To intuitively give some comparisons on the training performances of GANs, we use the artificial data following Gaussian distribution $\mathcal{N}(\mu = 4, \sigma = 1.25)$ to train the MIM-based GAN, original GAN, LSGAN and WGAN.

In particular, we first train the adversarial networks for a number of iterations (e.g. 500, 1,000 and 1,500 training iterations) to obtain a not bad discriminator. During each iteration, there are 16,000 samples produced by programming as initial input data for the discriminator. Then, with the fixed discriminator, a generator is trained by reducing the error of objective function in each kind of adversarial networks. Furthermore, we adopt two Deep Neural Networks (DNNs) as the generator and discriminator respectively, in which the Stochastic Gradient Descent (SGD) optimizer with 0.001 learning rate is chosen and the activation functions of discriminator and generator are sigmoid and tanh function respectively. Finally, we draw the error curves of the objection functions of generators to show the different performance during the training process.

2) Anomaly detection experiment based on MNIST and ODDS:

When detecting anomalies in the MNIST and ODDS, we adopt the general framework of GANs described in Section III-B1. However, to compare the efficiency of the GANs, including the original GAN, MIM-based GAN, LSGAN and WGAN, we change the main component (namely different objective functions for the data generation) of the framework. The Receiver Operating Characteristic (ROC) curve, Area Under Curve (AUC) and F_1 -score are used as criterions to compare different GANs for anomaly detection in the above datasets.

In details, the detection procedure on the MNIST and ODDS is similar to that mentioned in Section III-B1, where the neural networks training of GANs is the key point. At first, as for the framework of neural networks, DNNs are used, whose activation functions in the output layers are sigmoid function

and tanh function for the discriminator and generator respectively and those in the other layers are all leaky ReLU. Moreover, the Adam algorithm is chosen to optimize the weights for the networks with 0.001 learning rate. According to the properties of MNIST and ODDS, we configure the hidden layer size 256 for the MNIST and Musk dataset (belonging to the ODDS) as well as 64 for the Cardiocography and Thyroid in the ODDS. Furthermore, when we obtain trained GANs and the corresponding generative data, we use Eq. (23) and Eq. (25) (where $\lambda = 0.1$ and $\eta = 0.05$) to gain anomaly scores for testing data, in which the optimal z_{opt} in latent space is obtained by used of Adam optimizer with learning rate 0.003. At last, we adopt Eq. (21) to label the testing data so that the outliers (namely anomalies) are detected.

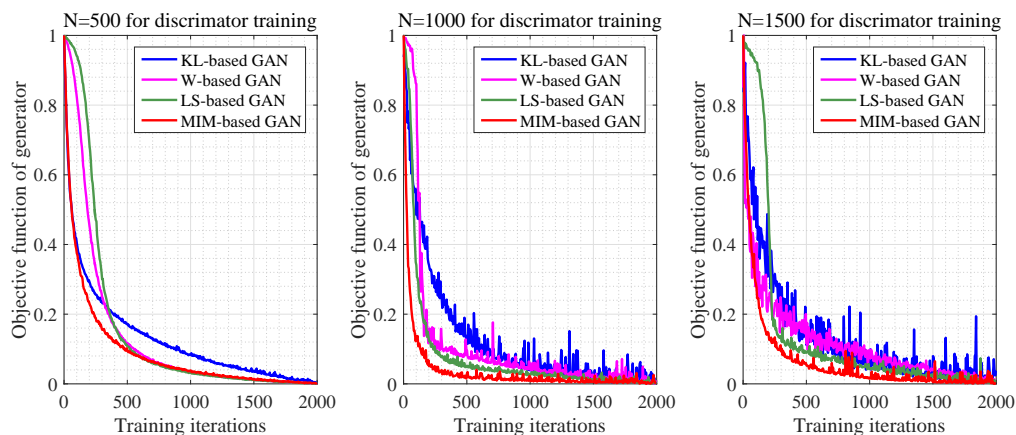


Fig. 1. The MIM-based GAN, KL-based GAN (namely original GAN), LS-based GAN (namely LSGAN) and W-based GAN (namely WGAN) are used to generate the data following Gaussian distribution $\mathcal{N}(\mu = 4, \sigma = 1.25)$ where μ and σ denote the mean value and the standard deviation value respectively. There are 16,000 input samples following the Gaussian distribution in every training iteration. The generators are trained with the discriminators fixed for 500, 1,000 or 1,500 training iterations (namely $N = 500, 1,000$ or $1,500$). In these cases, the curves for the objection functions of generators are drawn to compare the performances on training process.

C. Results and discussion

According to the above design for experiments, we do simulations with Pytorch and Matlab to evaluate the theoretical analysis. In particular, the experiment results are discussed as follows.

1) Training performance of GANs:

From figure 1, it is illustrated that during the training process, the MIM-based GAN, LSGAN and WGAN all perform better than the original GAN in the aspects of convergence and stability of training process. While, the MIM-based GAN also has its own superiority. On one hand, the MIM-based GAN has better convergence than the other GANs with respect to the objective function of generator. On the other hand, when a discriminator is given, the generator for MIM-based GAN has more stability than that

for original GAN, which is also comparable to those for LSGAN and WGAN. In brief, the MIM-based GAN converges to equilibrium faster and more stably than the original GAN. It also has these advantages on the training process to some degree, compared with LSGAN and WGAN.

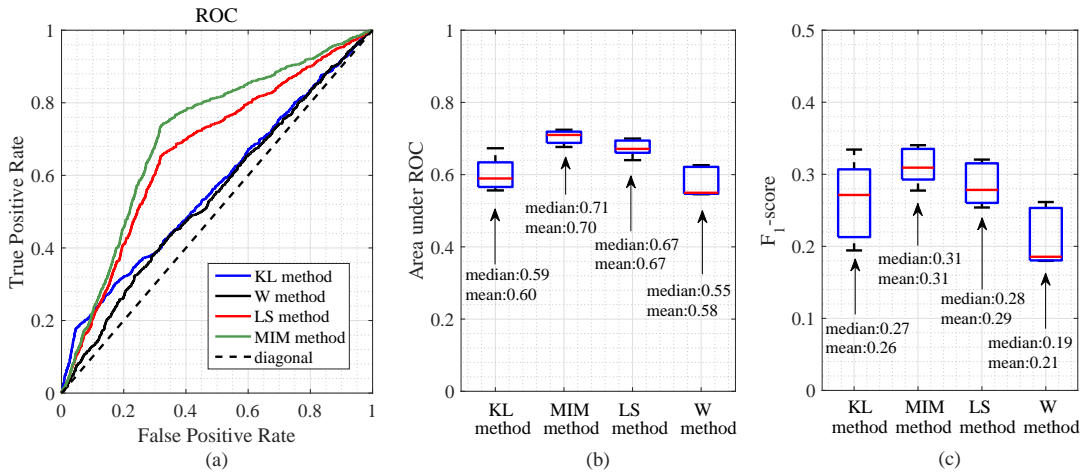


Fig. 2. ROC curve, AUC and F_1 -score for GAN-based anomaly detection in MNIST dataset, where MIM-based GAN (corresponding to MIM method), original GAN (corresponding to KL method), LSGAN (corresponding to LS method) and WGAN (corresponding to W method) are used to generate data.

2) Results of anomaly detection for MNIST and ODDS:

Figure 2 shows the performance of anomaly detection with different GANs in the MNIST experiment, including ROC curve, AUC and F_1 -score. In general, it is not difficult to see that the MIM-based GAN improves these kinds of performance compared with the other GANs. This is resulted from the fact that MIM-based objective function enlarges the proportion of rare events. Moreover, we also see that the volatility of the detection results (shown by the AUC and F_1 -score) in the KL-based GAN and W-based GAN methods is greater than that in two other methods.

Figure 3, 4 and 5 compare several GAN-based detection methods in the case of ODDS by showing the performances in terms of ROC curve, AUC and F_1 -score. Although there exists different performance in the three datasets of ODDS, MIM-based GAN still performs better on the anomaly detection. Particularly, on one hand, the ROC curve for MIM-based GAN method is more close to the ideal than those for the other detection methods with GANs. On the other hand, as for the AUC and F_1 -score of detection results, the corresponding statistics (including the median and mean) have better results when using MIM-based GAN method as shown in the box-plots (b) and (c) in Figure 3, 4 and 5. Actually, these datasets from ODDS repository provide some convincing and realistic evidences for the advantage of MIM-based GAN

on anomaly detection.

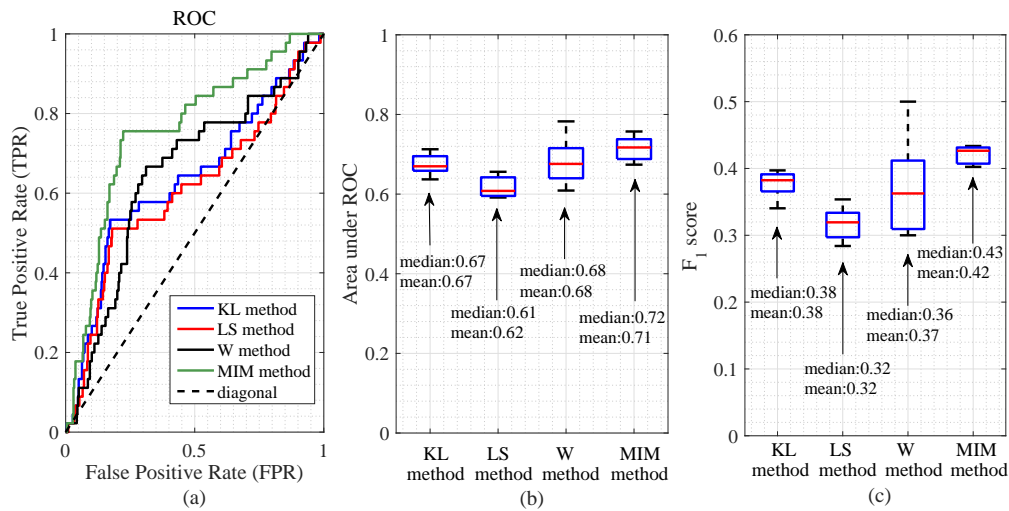


Fig. 3. ROC curve, AUC and F_1 -score for GAN-based anomaly detection in Cardiocotography dataset.

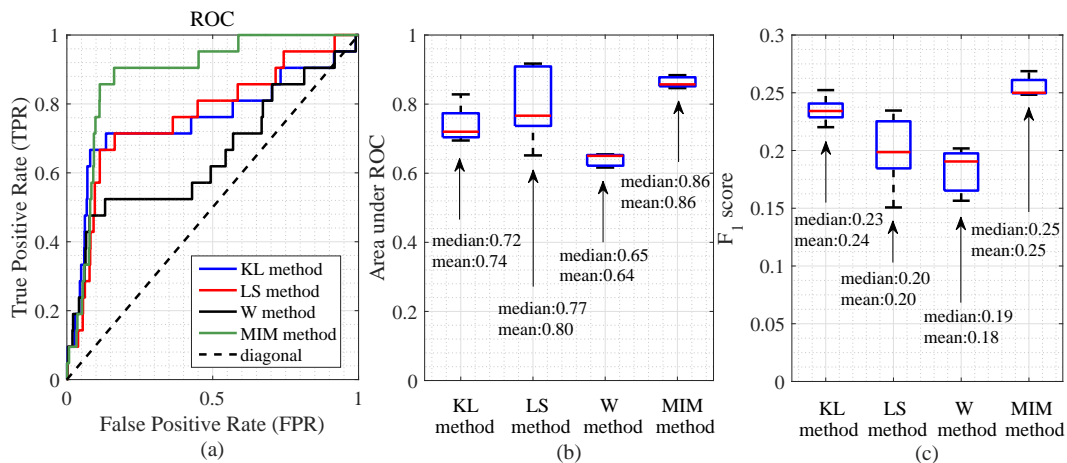


Fig. 4. ROC curve, AUC and F_1 -score for GAN-based anomaly detection in Thyroid dataset.

V. CONCLUSION

In this paper, we proposed a new model named MIM-based GAN to enrich the conventional GANs. In terms of this model, it has different performance of training process with the other classical GANs. Furthermore, another advantage of this new developed approach is to highlight the proportion of rare events in the objective function to generate more efficient data. In addition, we showed that compared with the classical GANs, the MIM-based GAN has more superiority on the anomaly detection, which may be a promising application direction with GANs in practice.

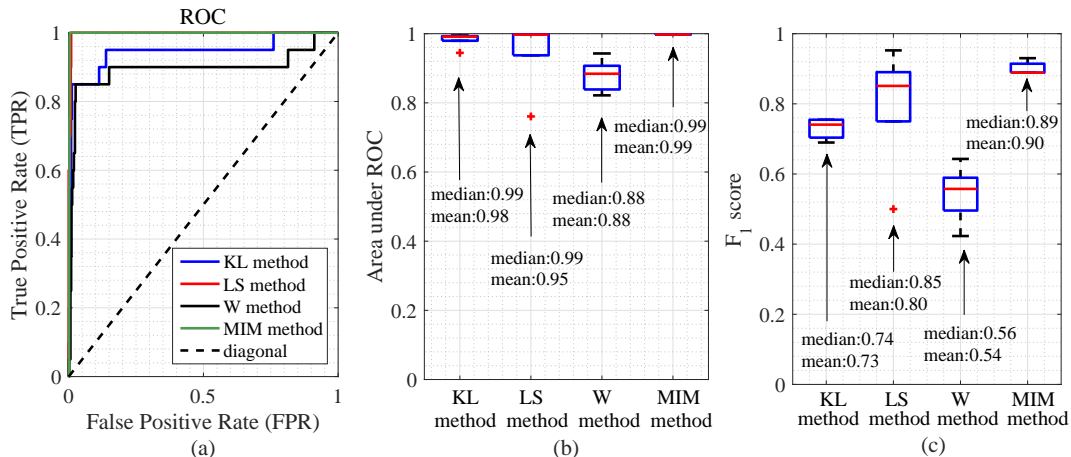


Fig. 5. ROC curve, AUC and F_1 -score for GAN-based anomaly detection in Musk dataset.

ACKNOWLEDGMENT

We thank a lot for the advices from Prof. Xiaodong Wang and Xiao-Yang Liu at Columbia University, USA. Their suggestions make a positive effect on this work.

APPENDIX A

PROOF OF COROLLARY 1

With respect to the MIM-based GAN, original GAN and its improved GAN, it is not difficult to see that the corresponding gradient functions of generators depend on $\nabla_{\theta} \mathbb{E}_{z \sim \mathbb{P}_z} [\exp(D(g_{\theta}(z)))]$, $\nabla_{\theta} \mathbb{E}_{z \sim \mathbb{P}_z} [\ln(1 - D(g_{\theta}(z)))]$ and $\nabla_{\theta} \mathbb{E}_{z \sim \mathbb{P}_z} [-\ln(D(g_{\theta}(z)))]$, respectively.

On one hand, in the case that $D - \tilde{D}^* = \epsilon$ ($\epsilon \in [0, 1]$ and $\tilde{D}^*(g_{\theta}(z)) = 0$), we have

$$\begin{aligned}
 \nabla_{\theta} \mathbb{E}_{z \sim \mathbb{P}_z} [\ln(1 - D(g_{\theta}(z)))] &= \mathbb{E}_{z \sim \mathbb{P}_z} \left[-\frac{\nabla_{\mathbf{x}} D(\mathbf{x}) \nabla_{\theta} g_{\theta}(z)}{1 - D(g_{\theta}(z))} \right] \\
 &= \mathbb{E}_{z \sim \mathbb{P}_z} \left[-\frac{\nabla_{\mathbf{x}} D(\mathbf{x}) \nabla_{\theta} g_{\theta}(z)}{1 - \tilde{D}^*(g_{\theta}(z)) - \epsilon} \right] \\
 &= -\frac{1}{1 - \epsilon} \mathbb{E}_{z \sim \mathbb{P}_z} [\nabla_{\mathbf{x}} D(\mathbf{x}) \nabla_{\theta} g_{\theta}(z)],
 \end{aligned} \tag{27}$$

$$\begin{aligned}
 \nabla_{\theta} \mathbb{E}_{z \sim \mathbb{P}_z} [-\ln(D(g_{\theta}(z)))] &= \mathbb{E}_{z \sim \mathbb{P}_z} \left[-\frac{\nabla_{\mathbf{x}} D(\mathbf{x}) \nabla_{\theta} g_{\theta}(z)}{D(g_{\theta}(z))} \right] \\
 &= \mathbb{E}_{z \sim \mathbb{P}_z} \left[-\frac{\nabla_{\mathbf{x}} D(\mathbf{x}) \nabla_{\theta} g_{\theta}(z)}{\tilde{D}^*(g_{\theta}(z)) + \epsilon} \right] \\
 &= -\frac{1}{\epsilon} \mathbb{E}_{z \sim \mathbb{P}_z} [\nabla_{\mathbf{x}} D(\mathbf{x}) \nabla_{\theta} g_{\theta}(z)].
 \end{aligned} \tag{28}$$

It is not difficult to see that $\frac{1}{\epsilon}$ and $\frac{1}{1-\epsilon}$ are symmetric in the case $\epsilon \in [0, 1]$, which implies that $\nabla_{\theta} \mathbb{E}_{z \sim \mathbb{P}_z} [-\ln(D(g_{\theta}(z)))]$ has the same anti-interference ability as $\nabla_{\theta} \mathbb{E}_{z \sim \mathbb{P}_z} [\ln(1 - D(g_{\theta}(z)))]$.

As for the function $h(u) = \frac{1}{1-u} - \exp(u)$ ($u \in [0, 1]$), it is not difficult to see that $h(u) \geq 0$ for $u \in [0, 1]$ where the equation holds at $u = 0$. In fact, $\exp(-u) \geq 1 - u$ for $u \in [0, 1]$. Therefore, by comparing Eq. (12) with Eq. (27) and Eq. (28), it is readily seen that the result of this corollary is true.

On the other hand, in the case that $D - \check{D}^* = \epsilon$ ($|\epsilon| < \frac{1}{2}$ and $\check{D}^*(g_\theta(\mathbf{z})) = \frac{1}{2}$), it is not difficult to see that

$$\begin{aligned} \nabla_{\theta} \mathbb{E}_{\mathbf{z} \sim \mathbb{P}_z} [\ln(1 - D(g_\theta(\mathbf{z})))] &= \mathbb{E}_{\mathbf{z} \sim \mathbb{P}_z} \left[-\frac{\nabla_{\mathbf{x}} D(\mathbf{x}) \nabla_{\theta} g_{\theta}(\mathbf{z})}{1 - \check{D}^*(g_{\theta}(\mathbf{z})) - \epsilon} \right] \\ &= -\frac{1}{\frac{1}{2} - \epsilon} \mathbb{E}_{\mathbf{z} \sim \mathbb{P}_z} [\nabla_{\mathbf{x}} D(\mathbf{x}) \nabla_{\theta} g_{\theta}(\mathbf{z})], \end{aligned} \quad (29)$$

$$\begin{aligned} \nabla_{\theta} \mathbb{E}_{\mathbf{z} \sim \mathbb{P}_z} [-\ln(D(g_\theta(\mathbf{z})))] &= \mathbb{E}_{\mathbf{z} \sim \mathbb{P}_z} \left[-\frac{\nabla_{\mathbf{x}} D(\mathbf{x}) \nabla_{\theta} g_{\theta}(\mathbf{z})}{\check{D}^*(g_{\theta}(\mathbf{z})) + \epsilon} \right] \\ &= -\frac{1}{\frac{1}{2} + \epsilon} \mathbb{E}_{\mathbf{z} \sim \mathbb{P}_z} [\nabla_{\mathbf{x}} D(\mathbf{x}) \nabla_{\theta} g_{\theta}(\mathbf{z})]. \end{aligned} \quad (30)$$

It is readily seen that $\frac{1}{\frac{1}{2} - \epsilon}$ and $\frac{1}{\frac{1}{2} + \epsilon}$ are symmetric if there exists a small disturbance, i.e. $|\epsilon| < C < \frac{1}{2}$ (C is a constant), that is to say, the anti-interference ability for $\nabla_{\theta} \mathbb{E}_{\mathbf{z} \sim \mathbb{P}_z} [-\ln(D(g_\theta(\mathbf{z})))]$ is equal to that for $\nabla_{\theta} \mathbb{E}_{\mathbf{z} \sim \mathbb{P}_z} [\ln(1 - D(g_\theta(\mathbf{z})))]$.

Considering the function $h(u) = \frac{1}{\frac{1}{2} - u} - \exp(\frac{1}{2} + u)$ where $u \in (-\frac{1}{2}, \frac{1}{2})$, it is readily seen that $h(u) > 0$ for $u \in (-\frac{1}{2}, \frac{1}{2})$. Thus, by comparing Eq. (13) with Eq. (29) and Eq. (30), it is easy to see that the result of this corollary also is true.

To sum up, the corollary is verified.

REFERENCES

- [1] I. J. Goodfellow, J. Pouget-Abadie, M. Mirza, B. Xu, D. Warde-Farley, S. Ozair, A. Courville and Y. Bengio, ‘‘Generative adversarial nets’’, in *Proc. Advances in Neural Information Processing Systems (NeurIPS 2014)*, Montreal, Quebec, Canada, Dec. 8–13, 2014, pp. 2672–2680.
- [2] X. Mao, Q. Li, H. Xie, R. Lau, Z. Wang, and S. P. Smolley, ‘‘On the effectiveness of least squares generative adversarial networks,’’ *IEEE Trans. Pattern Anal. Mach. Intell.*, vol. 41, no. 12, pp. 2947–2960, Dec. 2019.
- [3] S. Wang, G. Peng, and Z. Zheng, ‘‘Capturing joint label distribution for multi-label classification through adversarial learning,’’ *IEEE Trans. Knowl. Data Eng.*, vol. 14, no. 8, pp. 1–12, Aug. 2015.
- [4] Y. Liu, Z. Li, C. Zhou, Y. Jiang, J. Sun, M. Wang and X. He ‘‘Generative adversarial active learning for unsupervised outlier detection,’’ *IEEE Trans. Knowl. Data Eng.*, early access, pp. 1–12, 2019.
- [5] T. Fernando, S. Denman, S. Sridharan, and C. Fookes, ‘‘Memory augmented deep generative models for forecasting the next shot location in tennis,’’ *IEEE Trans. Knowl. Data Eng.*, early access, pp. 1–12, 2019.
- [6] C. Ledig, L. Theis, F. Huszar, J. Caballero, A. P. Aitken, A. Tejani, J. Totz, Z. Wang and W. Shi, ‘‘Photo-realistic single image super-resolution using a generative adversarial network’’, in *Proc. IEEE Conference on Computer Vision and Pattern Recognition (CVPR 2017)*, Honolulu, HI, USA, Jul. 21–26, 2017, pp. 4681–4690.

- [7] A. Kuefler, J. Morton, T. A. Wheeler and M. J. Kochenderfer, “Imitating driver behavior with generative adversarial networks”, in *Proc. IEEE Intelligent Vehicles Symposium (IV 2017)*, Los Angeles, CA, USA, Jun. 11–14, 2017, pp. 204–211.
- [8] A. Shrivastava, T. Pfister, O. Tuzel, J. Susskind, W. Wang and R. Webb, “Learning from simulated and unsupervised images through adversarial training”, in *Proc. IEEE Conference on Computer Vision and Pattern Recognition (CVPR 2017)*, Honolulu, HI, USA, Jul. 21–26, 2017, pp. 2107–2116.
- [9] C. K. Sonderby, J. Caballero, L. Theis, W. Shi and F. Huszar, “Amortised map inference for image super-resolution”, in *Proc. International Conference on Learning Representations (ICLR 2017)*, Palais des Congres Neptune, Toulon, France, Apr. 24–26, 2017, pp. 1–17.
- [10] J. Zhao, M. Mathieu and Y. LeCun, “Energy-based generative adversarial networks”, in *Proc. International Conference on Learning Representations (ICLR 2017)*, Palais des Congres Neptune, Toulon, France, Apr. 24–26, 2017, pp. 1–16.
- [11] X. Mao, Q. Li, H. Xie, R. Y. K. Lau, Z. Wang and S. P. Smolley, “Least squares generative adversarial networks”, in *Proc. IEEE International Conference on Computer Vision (ICCV 2017)*, Venice, Italy, Oct. 22–29, 2017, pp. 2794–2802.
- [12] Y. Mroueh and T. Sercu, “Fisher GAN”, in *Proc. Advances in Neural Information Processing Systems (NeurIPS 2017)*, Long Beach, CA, USA, Dec. 3–9, 2017, pp. 2513–2523.
- [13] S. Nowozin, B. Cseke and R. Tomioka, “f-GAN: Training generative neural samplers using variational divergence minimization”, in *Proc. Advances in Neural Information Processing Systems (NeurIPS 2016)*, Barcelona, Spain, Dec. 5–10, 2016, pp. 271–279.
- [14] M. Arjovsky, S. Chintala and L. Bottou, “Wasserstein GAN”, <https://arxiv.org/abs/1701.07875>, pp. 1–32.
- [15] I. Gulrajani, F. Ahmed, M. Arjovsky, V. Dumoulin and A. Courville, “Improved training of Wasserstein GANs”, in *Proc. Advances in Neural Information Processing Systems (NeurIPS 2017)*, Long Beach, CA, USA, Dec. 3–9, 2017, pp. 5767–5777.
- [16] H. Soleimani and D. J. Miller, “ATD: Anomalous topic discovery in high dimensional discrete data,” *IEEE Trans. Knowl. Data Eng.*, vol. 28, no. 9, pp. 2267–2280, Sep. 2016.
- [17] M. Radovanovic, A. Nanopoulos, and M. Ivanovic, “Reverse nearest neighbors in unsupervised distance-based outlier detection,” *IEEE Trans. Knowl. Data Eng.*, vol. 27, no. 5, pp. 1369–1382, May. 2015.
- [18] C. Oreilly, A. Gluhak, and M. A. Imran, “Adaptive anomaly detection with kernel eigenspace splitting and merging,” *IEEE Trans. Knowl. Data Eng.*, vol. 27, no. 1, pp. 3–16, Jan. 2015.
- [19] D. Li, D. Che, J. Goh, and S. Ng. “Anomaly detection with generative adversarial networks for multivariate time series”, in *Proc. ACM Knowledge Discovery and Data Mining Conference Workshops (KDD Wkshps 2018)*, London, United Kingdom, Aug. 19–23, 2018, pp. 1–10.
- [20] L. Deecke, R. Vandermeulen, L. Ruff, S. Mandt, and M. Kloft, “Image anomaly detection with generative adversarial networks”, in *Proc. Joint European Conference on Machine Learning and Knowledge Discovery in Databases (ECML-PKDD 2018)*, Dublin, Ireland, Sep. 10–14, 2018, pp. 3–17.
- [21] T. Schlegl, P. Seebock, S. M. Waldstein, U. Schmidt-Erfurth, and G. Langs, “Unsupervised anomaly detection with generative adversarial networks to guide marker discovery”, in *Proc. International Conference on Information Processing in Medical Imaging (IPMI 2017)*, Boone, North Carolina, USA, Jun. 25–30, 2017, pp. 146–157.
- [22] M. Ravanbakhsh, E. Sangineto, M. Nabi, and N. Sebe, “Training adversarial discriminators for cross-channel abnormal event detection in crowds”, in *Proc. IEEE Winter Conference on Applications of Computer Vision (WACV 2019)*, Hawaii, United States, Jan. 7–11, 2019, pp. 1896–1904.
- [23] H. Zenati, C. S. Foo, B. Lecouat, G. Manek, and V. R. Chandrasekhar, “Adversarially learned anomaly detection”, in *Proc. IEEE International Conference on Data Mining (ICDM 2018)*, Singapore, Singapore, Nov. 17–20, 2018, pp. 727–736.
- [24] P. Isola, J. Y. Zhu, T. Zhou and A. A. Efros, “Image-to-image translation with conditional adversarial networks,” in *Proc. IEEE Conference on Computer Vision and Pattern Recognition (CVPR 2017)*, Honolulu, HI, USA, Jul. 21–26, 2017, pp. 1125–1134.

- [25] J. Donahue, P. Krahenbuhl, and T. Darrell, “Adversarial feature learning”, in *Proc. International Conference on Learning Representations (ICLR 2017)*, Palais des Congres Neptune, Toulon, France, Apri. 24–26, 2017, pp. 1–18.
- [26] T. Schlegl, P. Seebock, S. M. Waldstein, G. Langs and U. Schmidt-Erfurth, “f-AnoGAN: Fast unsupervised anomaly detection with generative adversarial networks”, *Medical Image Analysis*, vol. 54, pp. 30–44, May 2019.
- [27] A. Odena, V. Dumoulin and C. Olah. “Deconvolution and checkerboard artifacts”, *Distill*, vol. 1, no. 10, Oct, 17, 2016, <http://distill.pub/2016/deconv-checkerboard>
- [28] D. Lopez-Paz and M. Oquab. “Revisiting classifier two-sample tests”, in *Proc. International Conference on Learning Representations (ICLR 2017)*, Palais des Congres Neptune, Toulon, France, Apri. 24–26, 2017, pp. 1–15.
- [29] P. Fan, Y. Dong, J. X. Lu, and S. Y. Liu, “Message importance measure and its application to minority subset detection in big data”, in *Proc. IEEE Globecom Workshops (GC Wkshps 2016)*, Washington D.C., USA, Dec. 4–8, 2016, pp. 1–6.
- [30] S. Liu, R. She, and P. Fan, “Differential message importance measure: A new approach to the required sampling number in big data structure characterization”, *IEEE Access*, vol. 6, pp. 42851–42867, Jul. 2018.
- [31] S. Liu, R. She, P. Fan, and K. B. Letaief. “Non-parametric message important measure: Storage code design and transmission planning for big data”, *IEEE Trans. Commun.*, vol. 66, no. 11, pp. 5181–5196, Nov. 2018.
- [32] R. She, S. Y. Liu, and P. Fan, “Amplifying inter-message distance: On information divergence measures in big data”, *IEEE Access*, vol. 5, pp. 24105–24119, Nov. 2017.